Proton MR Spectroscopy of Squamous Cell Carcinoma of the Extracranial Head and Neck: In Vitro and In Vivo Studies

Suresh K. Mukherji, Sharon Schiro, Mauricio Castillo, Lester Kwock, Keith E. Muller, and William Blackstock

PURPOSE: To determine the ability of in vitro one-dimensional and two-dimensional proton MR spectroscopy to help differentiate squamous cell carcinoma of the extracranial head and neck from normal tissues and to correlate the in vitro observations with clinical studies. **METHODS**: In vitro 1-D and 2-D correlated proton MR spectroscopy (11 T) was performed in tissue specimens of squamous cell carcinoma of the head and neck (n = 19), in normal tissue (n = 13), in metastatic cervical lymph nodes (n = 3), and in a squamous cell carcinoma cell line. In vivo 1-D proton MR spectroscopy (1.5 T) was performed in patients with squamous cell carcinoma (n = 7) and in healthy volunteers (n = 7). The ratio of the areas under the choline (Cho) and creatine (Cr) resonances were calculated for 1-D proton MR spectra for the in vitro tissue studies and correlated with the in vivo studies. Data from in vitro 2-D correlated spectroscopy were analyzed for differences in the presence or absence of various metabolites in samples of tumor and normal tissue. Statistical analysis consisted of 2×2 factorial repeated measures analysis of variance (ANOVA), discriminate analysis, and χ^2 test. **RESULTS:** The mean in vitro 1-D proton MR spectroscopic Cho/Cr ratio was significantly higher in tumor than in normal tissue. The difference between the mean ratios appeared to increase with increasing echo time. All in vivo tumor Cho/Cr ratios were greater than the calculated mean in vitro tumor ratio, whereas six of the seven volunteers had no detectable Cho and Cr resonances. Two-dimensional correlated MR spectroscopic data revealed that a variety of amino acids have a significantly greater likelihood of being detected in tumor than in normal tissues. **CONCLUSIONS:** One-dimensional and 2-D proton MR spectroscopy can help differentiate primary squamous cell carcinoma and nodal metastases containing squamous cell carcinoma from normal tissue both in vitro and in vivo. In addition, 2-D spectroscopy can help identify the presence of certain amino acids in squamous cell carcinoma that are not detected in normal tissue.

Index terms: Magnetic resonance, spectroscopy; Carcinoma; Neck, neoplasms

AJNR Am J Neuroradiol 18:1057–1072, June 1997

Magnetic resonance (MR) spectroscopy has the unique ability to depict tissues at a cellular level noninvasively. Both phosphorous-31 (^{31}P) and proton MR spectroscopy have been used for research and clinical purposes. Recent investigations have evaluated the role of proton MR spectroscopy for a variety of oncologic applications. Proton MR spectroscopic analysis has been done for a variety of malignant conditions, including colon, prostate, breast, gynecologic, and various intracranial neoplasms (1–6) (W. Negendank, R. Zimmerman, E. Gotsis, et al, "A Cooperative Group Study of 1H MRS of Primary Brain Tumors" (abstract), presented at the annual meeting of the Society of Magnetic Resonance in Medicine, 1993; and A. A. Tzika, P. D. Barnes, N. J. Tarbell, et al, "Spectroscopic and Hemodynamic MR Characterization of Pediatric Brain Tumors" (abstract), presented at the annual meeting of the Radiological Society of North America, Chicago, Ill, November 1995).

Both ^{31}P and proton MR spectroscopy have been used to identify differences in metabolite

Received April 10, 1996; accepted after revision January 13, 1997.

From the Departments of Radiology (S.K.M., S.S., M.C., L.K.) and Radiation Oncology (W.B.), University of North Carolina School of Medicine, and the Department of Biostatistics, University of North Carolina School of Public Health (K.E.M.), Chapel Hill.

Address reprint requests to Suresh K. Mukherji, MD, Department of Radiology, 3324 Infirmary CB# 7510, University of North Carolina School of Medicine, Chapel Hill, NC 27599.

AJNR 18:1057–1072, Jun 1997 0195-6108/97/1806–1057

concentrations in malignant and benign tissues (7–11). These studies have suggested that there are metabolites present in higher concentrations in malignant tumors than in surrounding normal tissues and that proton MR spectroscopy may be useful for distinguishing between them. Prior investigations have shown that intracranial astrocytomas have a higher choline/creatine (Cho/Cr) ratio than normal brain tissue (6, 7, 10)(Negendank et al, "A Cooperative..."; Tzika et al, "Spectroscopic..."). A similar pattern between squamous cell carcinomas arising from the upper aerodigestive tract and that seen in malignant brain tumors has been suggested (11–13).

We analyzed the metabolic profile of extracranial head and neck squamous cell carcinoma using both one-dimensional and two-dimensional correlated proton MR spectroscopy. The objectives of our study were as follows: 1) to determine differences in metabolic profiles between tumor and normal tissue by analyzing data from 1-D and 2-D correlated MR spectroscopy; 2) to ascertain whether proton MR spectroscopy can help differentiate tumor from uninvolved tissue on the basis of in vitro spectral analysis performed on tissue specimens and cell cultures analyzed at high field strengths (11 T); and 3) to correlate the data obtained from in vivo and in vitro 1-D proton MR spectroscopic studies.

Materials and Methods

In vitro 1-D and 2-D correlated proton MR spectroscopic analysis was performed on tissue specimens obtained from primary tumors (n = 19), metastatic cervical lymph nodes containing metastatic tumor (n = 3), and normal tissues (n = 13) at a high field strength (11 T). The same analysis was also performed on a human squamous cell carcinoma cell line culture established at our institution. The in vitro findings were correlated with the in vivo data obtained from patients with squamous cell carcinoma of the extracranial head and neck (n = 7) and with that from healthy volunteers (n = 7).

In Vitro Proton MR Spectroscopic Tissue Analysis

Tissue specimens from both squamous cell carcinoma (n = 19) and normal tissues (n = 13) in the neck were obtained as part of a tissue procurement protocol approved by the Institutional Review Board at our institution. Thirteen of 19 tumor samples were from newly diagnosed primary malignant lesions, whereas six of 19 tumor specimens were obtained from recurrent tumors that had previously been treated with surgery and/or radiation therapy. Nodal recurrences were not included in this portion of the study. All specimens (both primary and recurrent lesions) had arisen from the upper aerodigestive tract and were obtained from specimens that were histologically confirmed to consist of squamous cell carcinoma.

Normal tissues mostly consisted of muscle samples and small volumes of mucosa that were obtained with each resected specimen. These tissue samples were not directly adjacent to the tumors and did not affect surgical margins. We were unable to analyze samples composed purely of normal mucosa because of insufficient sample size. The tissue obtained from oral cavity or oropharynx consisted of tongue base musculature. Tissue from the strap muscles was obtained in cases of laryngeal, hypopharyngeal, and esophageal carcinoma.

One to 2 mL of tumor (n = 19) and normal tissue (n = 13) were obtained from surgical specimens at the time of resection. Normal tissue samples could not be obtained in all cases owing to the size of the lesion or margins of resection. All specimens were placed in plastic vials and immediately snap frozen in liquid nitrogen to preserve the metabolites. Samples were then stored in a −80°C freezer until the time of MR spectral analysis. In preparation for proton MR spectroscopy, the samples were thawed to room temperature, minced, and washed three times with D_2O phosphate-buffered saline to remove as much residual water as possible. Tissue samples were then placed on glass wool plugs (saturated with D_2O) in 5-mm nuclear MR tubes so that the tissues would be positioned between the coils of the proton probe. The temperature of the sample was maintained at 37°C in the MR probe during spectral acquisition.

Lymph Nodes.—Tissue specimens were obtained from cervical lymph nodes (n = 3) containing metastases from squamous cell carcinoma of the upper aerodigestive tract. The tissue was procured in a similar manner as described above. Metastatic lymph node specimens were analyzed in vitro using high-field proton MR spectroscopy (11 T) in the manner described above. One node per patient was analyzed. Specimens were obtained from nodes that contained obvious metastases on the basis of clinical and computed tomographic (CT) criteria (>1.5 cm in diameter with a low-attenuation center). The specimens used for proton MR spectroscopy consisted of solid nodal tissue without gross evidence of necrosis.

We were unable to analyze normal or indeterminate cervical lymph nodes because, in order to obtain sufficient tissue for adequate analysis, an entire node would have had to be removed, and removal of such a node would have prevented complete evaluation of the neck dissection and potentially interfered with the staging of the cancer.

Cell Culture.—In vitro 1-D and 2-D MR spectroscopy was performed in a human squamous cell carcinoma cell culture line (UNC-10), which was established through a tissue culture facility at our institution in collaboration with Glaxo Pharmaceuticals. The primary culture was obtained from a patient with poorly differentiated squamous cell carcinoma of the tongue base.

The UNC-10 cells were maintained as a monolayer culture in T-175 flasks containing RPMI-1640 medium supplemented with 5% fetal calf serum. Cells were harvested by mechanically scraping the cells from the flasks. The harvested cells were then centrifuged for 5 minutes (1000 rpm) and the pellet resuspended in D_2O phosphate-buffered saline (pD = 7.4) and repelleted. This step was performed twice. Finally, the cell pellet was resuspended in 10 mL of D_2O phosphate-buffered saline and allowed to equilibrate for 15 minutes at 37°C before cells again were spun down. Once the cells had been washed three times and pelleted, they were resuspended in a 1-mL volume of D_2O phosphate-buffered saline and placed in a 5-mm MR tube.

Spectral analysis was performed on two samples of the squamous cell carcinoma cell culture. The Cho/Cr ratios were measured for each sample and the average of the Cho/Cr area ratio was calculated. Two-dimensional correlated MR spectroscopy was performed on the cell culture samples to ascertain the presence or absence of the same metabolites that were analyzed in the in vitro tissue specimens and lymph nodes.

In Vitro 1-D and 2-D Spectroscopic Technique

MR proton spectra of excised tumors (n = 19), normal tissue (n = 13), metastatic lymph nodes (n = 3), and cell culture were obtained on a 500-MHz pulsed MR spectroscopic system in 5-mm tubes maintained at 37°C. The water signal was suppressed using a presaturation pulse centered over the water frequency.

In Vitro 1-D Proton MR Spectroscopy.—One-dimensional proton MR spectra were obtained with a Carr-Purcell-Meiboon-Gill sequence with data acquired at echo times (TEs) of 136 and 272 over a width of 7042.25 Hz (14.0806 ppm) using 8192 data points and 128 averages. Acquisition time was 0.582 second, and repetition time (TR) was 2000. An exponential line broadening of 5.00 Hz was applied to 1-D time domain data before Fourier transformation. The spectra were phase corrected (zero-order phase correction) to obtain the final spectra for analysis. Echo times of 136 and 272 were chosen because these are typically used for localized clinical MR spectroscopy at our institution.

Two-dimensional Correlated Spectroscopy.—Two-dimensional correlated MR spectroscopy provides a detailed analysis of metabolite resonances when compared with that obtained from standard 1-D MR spectroscopy. Two-dimensional correlated MR spectroscopy is an in vitro technique that allows additional separation of composite 1-D spectral MR resonances by generating crosspeaks in a second dimension, which identifies those protons that are spin-coupled (14). By providing coordinates of the crosspeaks, 2-D correlated MR spectroscopy allows for separation of similar metabolites that may be clustered under a single 1-D peak. The off-diagonal crosspeaks show which resonances on the diagonal are scalar coupled and hence allow these resonances to be assigned to specific molecules or compounds (15–17).

Two-dimensional correlated MR spectroscopy was performed on the in vitro samples (tissue specimens, cell culture, and lymph nodes). A total of 2000 data points were collected in the T2 time domain over a spectral width of 7042.253 Hz (14.0806 ppm). Data sampling was conducted with an initial delay between the two 90° pulses (T1 = 30 milliseconds, increment time = 3 milliseconds, and relaxation delay = 2 seconds). The number of time domain points collected in T1 was equal to 256 with eight averages over 72 minutes.

Two-dimensional correlated MR spectroscopic data matrices were zero filled to 1000 in T1, and Fourier transformation and magnitude calculations were performed to give 1024 × 1024 real data points for each 2-D correlated MR spectrum. Sine-bell window functions were applied uniformly in the T1 domain and lorentzian-gaussian window functions were applied in the T2 domain before Fourier transformation, as described by Delikatny et al (1). Assignment of 2-D crosspeaks was based on previously reported results by Lean et al (14).

In Vivo Clinical Studies

Seven patients with histologically proved squamous cell carcinoma of the upper aerodigestive tract and seven healthy volunteers underwent proton MR spectroscopy. Of the seven patients with tumors, six had primary lesions and one had recurrent disease. In six of the seven volunteers, spectra were obtained from the tongue base; in the other, spectra were obtained from the deep neck musculature.

Studies were performed on a Philips 1.5-T Gyroscan or Siemens 1.5-T SP unit. All patients were placed in the supine position with their head in a standard head coil. Because of limitations imposed by the use of the head coil, only tumors situated in the oral cavity, oropharynx, and nasopharynx were evaluated; laryngeal or hypopharyngeal lesions were not analyzed. Informed consent was obtained from all patients as part of a solid tumor protocol approved by the Institutional Review Board at our institution.

The area of tissue examined was identified from T1-weighted images acquired using a spin-echo sequence (600/30/1) with 5-mm-thick sections, a 0.5-mm gap, and a 256 × 256 matrix. In vivo proton MR spectroscopy was performed using the point-resolved spectroscopic (PRESS) location technique (136/2000/256 on the Phillips 1.5-T system, or 136/1600/256 on the Siemens 1.5-T system). Water suppression was achieved either by the water elimination Fourier transform technique, which uses a 180° inversion pulse sequence centered over the water resonance (Phillips 1.5-T system), or by means of a water saturation pulse sequence, which uses a low-powered gaussian pulse centered over the water resonance (chemical-shift selective saturation, Siemens 1.5 T). The shim in all cases was no greater than 0.2 ppm. In patients with tumors, a 2 × 2 × 2-cm volume of interest was placed over the tumor. In the volunteers, the same size volume was placed over the oral tongue (n = 6) or deep neck musculature (n = 1).

Statistical Analysis

One-dimensional Proton MR Spectroscopy.—Peak areas under the Cho (3.2 ppm) and Cr (3.02 ppm) resonances were estimated in all cases as the product of the peak height (PH) and the linewidth at half maximum height (FWHM). Peak heights were determined relative to a flat baseline drawn manually through the noise. The analysis was based on the assumption that the shape of each resonance approximated a gaussian density function. The properties of a gaussian function allow the area under the curve (AUC) for a particular resonance to be expressed as $AUC = PH \times FWHM \times \sqrt{\pi/4(\ln_e 2)}$. In turn, the Cho/Cr ratio for the area under the curves (R) can be calculated as follows: $R = PH_{Cho} \times FWHM_{Cho}/(PH_{Cr} \times FWHM_{Cr})$. These calculations were performed for the 1-D proton MR spectra of the in vitro studies (tumor and normal tissue samples, cell culture, and lymph nodes) and the in vivo studies (patients with squamous cell carcinoma and healthy volunteers). Cho/Cr ratios were determined for TEs of 136 and 272 for the in vitro experiments and for a TE of 136 for the in vivo studies. All measurements were made by a single observer who was aware of the origin of the spectra.

The Cho/Cr ratios (R) obtained from direct measurements of the specific Cho and Cr resonances were logarithmically transformed using the following formula: $Y = \log_{10}R$. This helped ensure the validity of the assumption of gaussian errors with constant variance necessary for accurate analysis of variance (see the Appendix for further discussion). Positive Y values correspond to $AUC_{Cho} > AUC_{Cr}$ and negative values correspond to $AUC_{Cho} < AUC_{Cr}$. A Y value of 1 corresponds to $AUC_{Cho} = AUC_{Cr}$.

To summarize, the statistical analyses were performed after a logarithmic transformation of the Cho/Cr ratio was applied in order to assure the validity of the statistical analyses. The Cho/Cr ratios mentioned in the "Results" section represent the antilog of the Y values calculated after the appropriate statistical analysis.

We attempted to determine whether there was a difference between the Cho/Cr ratios in tumor and normal tissues measured in vitro and whether the difference between the ratios changed with TE. To accomplish this, the Y value was calculated for the in vitro tumor and normal tissue specimens obtained at TEs of 136 and 272. The difference between the Cho/Cr ratio obtained at TEs of 136 and 272 performed on the same sample represents a repeated measures dimension. A 2×2 factorial repeated measures analysis of variance (ANOVA) was conducted for the data from each TE (136, 272) and tissue type (tumor, normal tissues).

An exploratory discriminant analysis was conducted to assess the potential utility of classifying tissue on the basis of the Cho/Cr ratio. A "linear" discriminant analysis was used, which assumed equal variance in each group. The use of the log transformation helped ensure the reasonableness of this assumption. Assuming equal prior probabilities of tumor or muscle, a cut point equal to the midpoint between the means was calculated. The sensitivity, specificity, positive predictive value (PPV), and negative predictive value (NPV) were calculated separately for the cut points for the in vitro 136 and 272 TE data. A tumor probability based on calculated Cho/Cr ratios was then derived for the in vitro data for TEs of both 136 and 272.

Last, we described the observed differences between the Cho/Cr ratios of the in vitro tumor specimens, the in vitro normal tissue specimens, and the in vivo tumor specimens. To maintain consistency with the previously described analyses, the Y variable was computed for a TE of 136 for the three tissue groups.

Two-dimensional Correlated MR Spectroscopy.—Two-dimensional correlated MR spectroscopic data were analyzed for the presence or absence of various metabolites. These metabolites were chosen because they had been identified in a variety of tumors by previous investigators (14–16). The metabolites examined in our study included Cho, phosphocholine, glycerophosphocholine, alanine, glycine, glutathione, glutamic acid, histidine, leucine, isoleucine, valine, inositol, taurine, lactate, and triglycerides (A,B,C,D,E,F,G_1,G_2,G') (2, 15). The shared crosspeaks of lysine/polyamine and fucose/threonine were also evaluated. The analysis was performed by a single observer who was unaware as to whether the 2-D correlated MR spectroscopic data belonged to tumor or normal tissue. Statistical analysis was performed using χ^2 analysis. A P value of less than .05 was considered significant.

Results

In Vitro Proton MR Spectroscopic Tissue Analysis

One-dimensional Proton MR Spectroscopy (Figs 1 and 2).—Our results show that the mean Cho/Cr ratios were significantly higher for tumors than for normal tissues ($P < .05$). This difference was detected for TEs of 136 and 272. The Y values and standard deviations are summarized in Table 1. The following discussion is based on the antilog of Y, which equals Cho/Cr ratios that can be directly measured from the spectral resonances. No Cho resonance was detectable in one normal tissue sample. Therefore, this sample was not included in the analysis and reduced the number of analyzed normal tissue samples to 12. The distribution of the data at TEs of 136 and 272 and a summary of the percentiles are illustrated in Figures 3 and 4.

The observed Cho/Cr ratios calculated at a TE of 136 ranged from 0.82 to 3.84 for tumor and 0.53 to 2.14 for normal tissue (Fig 3). All statistical tests were based on means of the Y values, as in Table 1. The statistical test of the difference in mean Y value of tumor and normal tissue gave a P value of .012. The mean Y

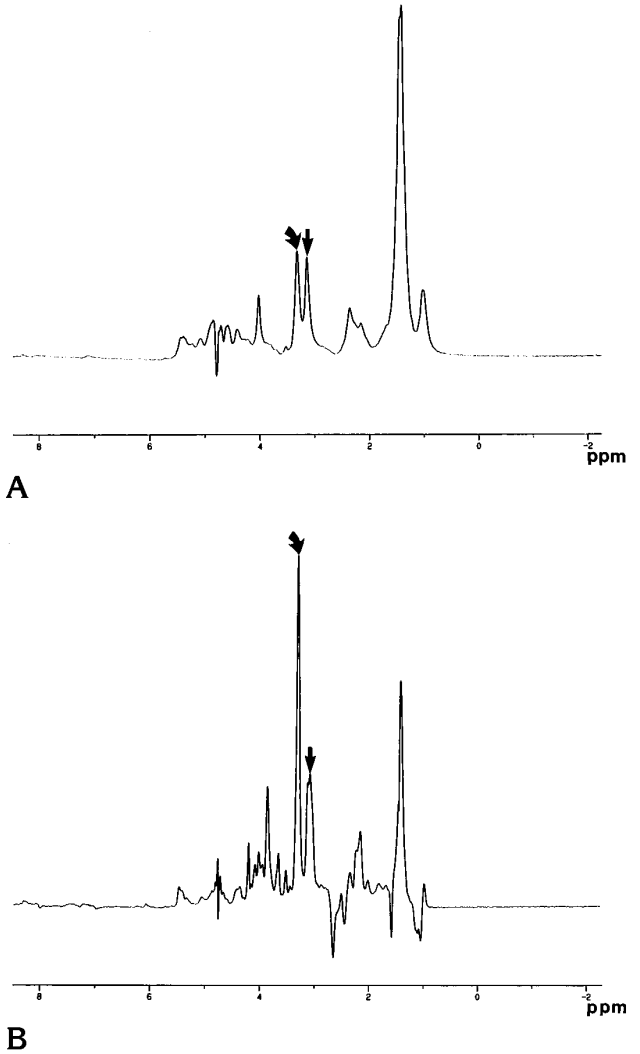

Fig 1. In vitro proton MR spectroscopy (2000/136).

A, Proton MR spectrum of normal tissue sample obtained from strap muscle shows similar areas of the Cho (*curved arrow*) and Cr (*straight arrow*) resonances. The Cho/Cr ratio is 1.06.

B, Proton MR spectrum of epiglottic squamous cell carcinoma tissue sample obtained from same patient as in *A* shows elevation of the Cho resonance (*curved arrow*) with respect to the Cr resonance (*straight arrow*). The Cho/Cr ratio is 1.92.

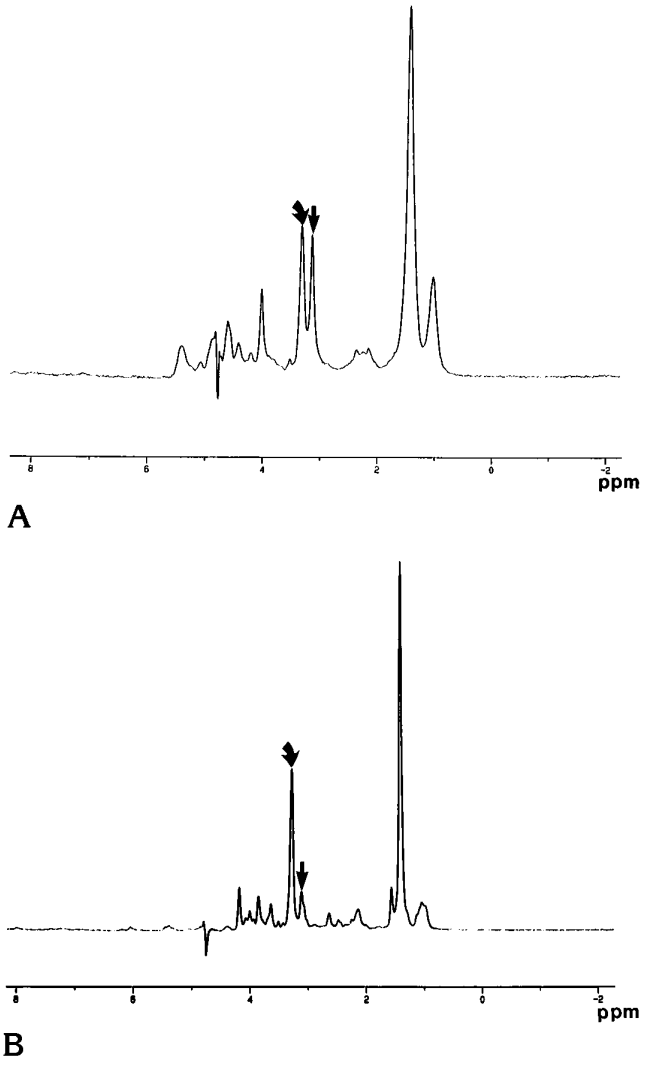

Fig 2. In vitro proton MR spectroscopy (2000/272).

A, Proton MR spectrum of the same normal tissue sample shown in Fig 1A obtained with a TE of 272. Cho (*curved arrow*) and Cr (*straight arrow*) resonances have similar appearance to those in Fig 1A. The Cho/Cr ratio is 1.06.

B, Proton MR spectrum of the same squamous cell carcinoma tissue sample shown in Fig 1B shows elevation of the Cho/Cr obtained at a TE of 272 (4.4) compared with the spectrum obtained at a TE of 136 (1.92) (compare with Fig 1B). Also note the marked difference in Cho/Cr ratio as compared with that in the normal tissue sample obtained from the same patient (*A*).

values were .223 (tumor) and .065 (normal). The Cho/Cr ratios, which corresponded to these mean Y values, were 1.67 for tumor ($10^{0.223}$) and 1.16 for normal tissue ($10^{0.065}$).

Our results show that the difference between mean values of $Y = \log_{10}(\text{Cho/Cr})$ for tumor and normal tissue increased with an increase in TE (Fig 4). At 2000/272 (TR/TE), the mean tumor Y value was .389, corresponding to a Cho/Cr ratio of 2.45 ($10^{0.389}$), and the mean normal Y value was .117, which corresponded to a Cho/Cr ratio of 1.31 ($10^{0.117}$) (Table 1). This difference between the ratios for tumor and normal tissue obtained at a TE of 272 was statistically significant ($P = .0002$). Additionally, the increase in the difference between the mean values of $Y = \log_{10}(\text{Cho/Cr})$ between tumor and normal tissue as the TE was increased from 136 to 272 was also statistically significant ($P = .031$).

TABLE 1: Logarithmic transformation of the in vitro choline/creatine area ratios

	TE = 136 (SD)	TE = 272 (SD)
Tumor	0.223 (0.161)	0.389 (0.188)
Normal tissue	0.065 (0.156)	0.117 (0.136)

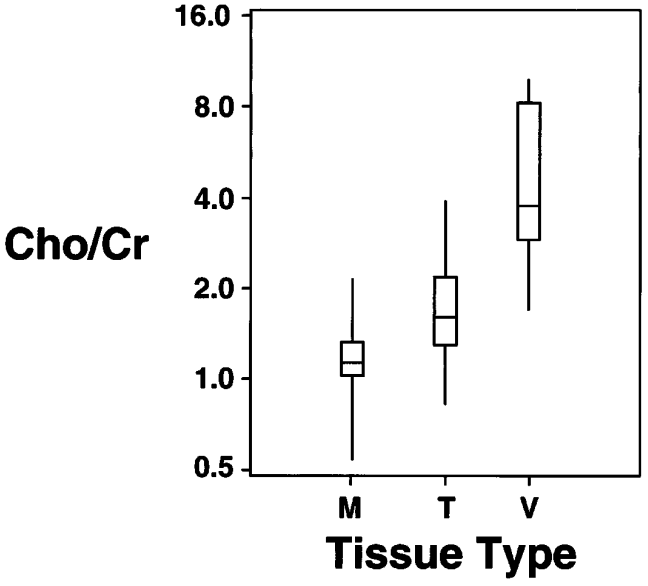

Fig 3. Box-and-whisker plot of the distribution of the Cho/Cr ratio obtained at a TE of 136 for in vitro normal tissue (*M*), tumor (*T*), and in vivo tumor (*V*). The box spans the range of Cho/Cr ratios from the 25th to 75th percentiles. The *bars* within the boxes indicate the median (50th percentile) Cho/Cr ratio. The *lines* ("whiskers") that extend above and below the boxes demarcate the maximum and minimum Cho/Cr ratios, respectively, for each group.

The in vitro tumor and normal tissue samples were analyzed by using discriminant analysis: $Y = \log_{10}(Cho/Cr)$ ratio was the discriminant variable. This analysis was performed for TEs of both 136 and 272. The cut points calculated for TEs of 136 and 272 were Cho/Cr ratios of 1.4 and 1.8, respectively. Twenty-three of the 31 samples were correctly assigned as either tumor or normal tissue on the basis of these cut points. Two samples were incorrectly classified as tumor and six were improperly classified as muscle. The results were identical for TEs of 136 and 272. Using this type of analysis, sensitivity was 68%, specificity was 88%, PPV was 87%, and NPV was 62%.

Using the above results, we calculated tumor probability on the basis of the Cho/Cr ratio. A plot of tumor probability as a function of the Cho/Cr ratio was constructed for TEs of both 136 and 272 (Fig 5). These data were plotted on a logarithmic scale because of the log transformation of the Cho/Cr ratio, which was initially performed to ensure a gaussian distribution of the errors for the observed values. The plot of the probabilities was S shaped (ogive) for TEs of both 136 and 272. The slope of the 272 TE curve was steeper than that of the 136 TE curve between the 20th and 80th percentiles, suggesting that the Cho/Cr ratio measured at a TE of 272 may provide better distinction between tumor and nonmalignant tissue (Fig 5).

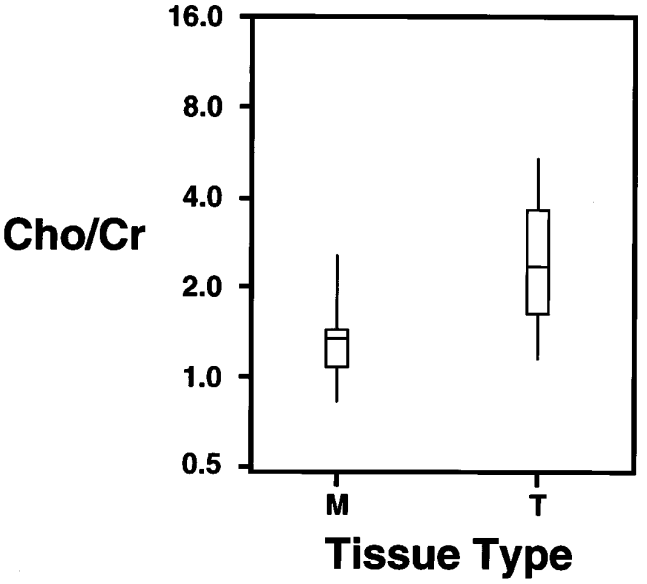

Fig 4. Box-and-whisker plot of the distribution of the Cho/Cr ratio obtained at a TE of 272 for in vitro normal tissue (*M*) and tumor (*T*).

Two-dimensional Correlated MR Spectroscopy.—A χ^2 analysis of the 2-D correlated MR spectroscopic data of tumor and normal tissue showed that a variety of amino acids have a significantly greater likelihood of being detected in tumor than in normal tissue; specifically, alanine, glutathione, histidine, isoleucine, valine, and the shared crosspeak for lysine/polyamine (Fig 6). Both alanine and isoleucine were detected in 15 of 19 tumor samples and found in only one of 13 samples of normal tissue. Glutathione, histidine, and valine were found in eight, 10, and 12 tumor samples, respectively, whereas each amino acid was detected in only one of 13 normal tissue samples. The shared crosspeak for lysine/polyamine (1.72 to 3.05 ppm) was present in all 19 tumors and in 10 of 13 normal tissue samples. These results are summarized in Table 2.

Cell Culture.—One-dimensional proton MR spectroscopy of squamous cell carcinoma cell culture revealed a markedly elevated Cho res-

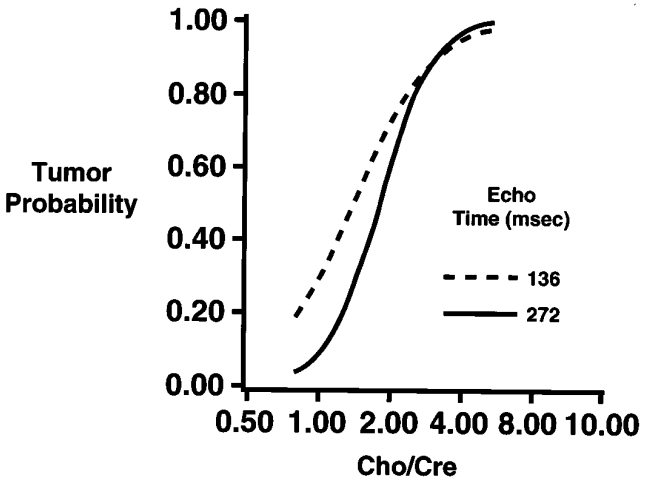

Fig 5. Plot of tumor probabilities based on Cho/Cr ratio. The curves have an S-shape configuration (ogive) and support the contention that the Cho/Cr ratio is an important metabolic marker for differentiating tumor from normal tissue. The greater slope of the 272 TE curve relative to the 136 TE curve between the 20th and 80th percentiles suggests that a longer TE may provide better distinction between tumor and normal tissue.

onance intensity as compared with Cr. The average Cho/Cr obtained at a TE of 136 was 3.25, which increased to 3.93 when the TE was increased to 272 (Fig 7).

Two-dimensional correlated proton MR spectroscopy also showed detectable levels of the polyamine/lysine shared crosspeak. The other amino acids that were found to be present in solid tumors (alanine, glutamate, histidine, isoleucine, and valine) were not detected in the tissue-cultured tumor cells.

Lymph Nodes.—The metastatic cervical lymph nodes had 1-D and 2-D proton MR spectra similar to that obtained from tumor tissue samples and cell culture. For the 1-D spectra, the Cho/Cr ratios at a TE of 136 were 1.94, 1.98, and 5.75 (mean, 3.22). This ratio was also dependent on TE. The Cho/Cr ratios increased to 2.25, 3.36, and 6.67, respectively (mean, 4.09), when TE was increased to 272 (Fig 8).

Two-dimensional correlated MR spectral analysis revealed that the amino acids present in significantly higher quantities in tumor tissue samples than in normal tissues were also present in involved lymph nodes. Alanine and the polyamine/lysine shared crosspeak were present in all three metastatic nodes whereas glutathione, histidine, isoleucine, and valine were present in two thirds of the involved nodes (Fig 9).

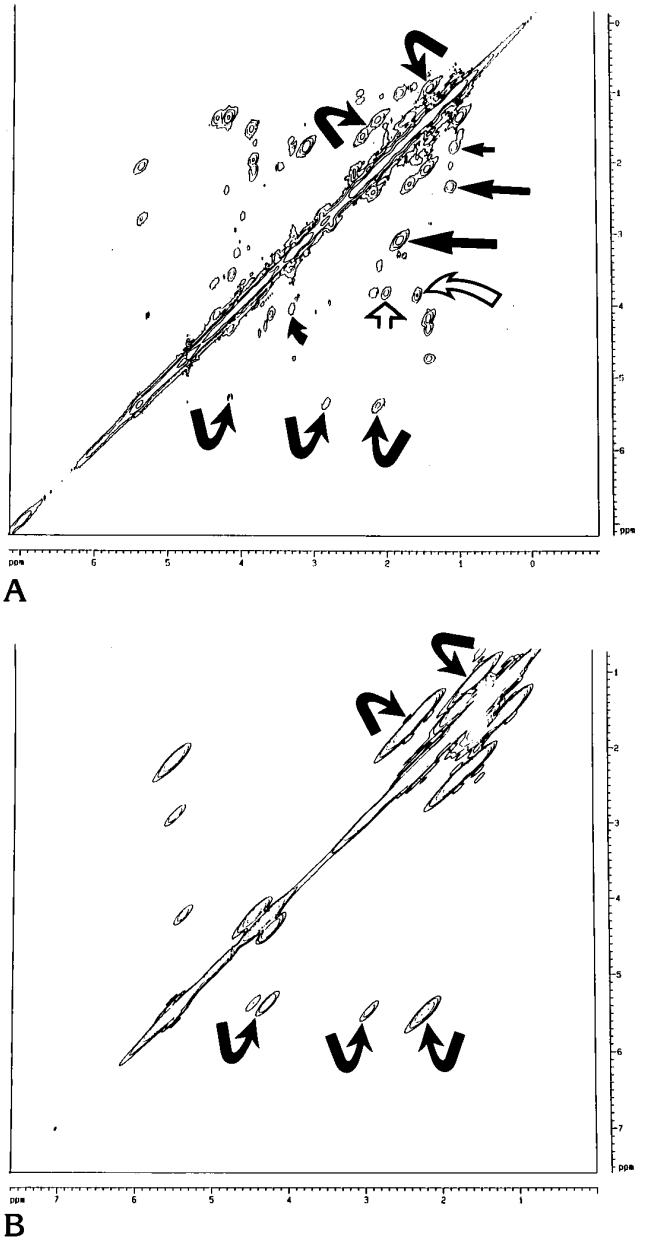

Fig 6. Two-dimensional correlated MR spectra of tumor sample (*A*) illustrate the multiple contours of the various metabolites that had a statistically greater likelihood of being detected in tumor than in normal tissue (*B*). These metabolites include alanine (*curved open arrow*), glutathione (*straight open arrow*), histidine (*small curved solid arrow*), isoleucine (*small straight solid arrow*), valine (*medium straight solid arrow*), and shared crosspeak for polyamine/lysine (*large straight solid arrow*). Notice the absence of these metabolites in the 2-D correlated MR spectra of the normal tissue sample (*B*). Also note the difference in the contours of the triglyceride resonances (*large curved solid arrows*). There is no significant difference between tumor and normal tissue as to presence or absence of the various triglycerides. However, the contours of the triglyceride peaks are noticeably different. These resonances appear elliptical in normal tissue (*large curved solid arrows* in *B*) whereas in tumor they are narrow and less elliptical owing to decreased chemical-shift dispersion (*A*).

TABLE 2: Metabolites detected within tumors versus normal tissue as analyzed with 2-D correlated proton MR spectroscopy

Metabolite	Crosspeak (ppm)	*P*
Alanine	1.49–3.79	0.001*
Glutathione	2.21–3.81	0.03*
Histadine	3.22–3.95	0.017*
Isoleucine	0.97–2.12	0.001*
Polyamine/lysine	1.72–3.05	0.028*
Valine	1.03–2.34	0.002*
Choline	3.50–4.07	0.108
Phosphocholine	3.61–4.25	0.185
Glutamic acid	2.21–2.62	0.11
Glycerophosphocholine	3.69–4.38	0.892
Leucine	0.97–1.78	0.401
Fucose/threonine	1.33–4.27	0.114
Inositol	3.28–3.64	0.463
Taurine	3.28–3.50	0.218
Lactate	1.33–4.12	0.135
Triglyceride A	0.90–1.33	0.227
Triglyceride B	1.33–2.08	0.975
Triglyceride C	2.02–5.38	0.597
Triglyceride D	2.84–5.38	0.719
Triglyceride E	1.33–1.62	0.185
Triglyceride F	1.60–2.30	†
Triglyceride G1	4.12–5.26	0.061
Triglyceride G2	4.26–5.26	0.604
Triglyceride G'	4.09–4.29	0.169

* Statistically greater likelihood of detecting the presence of metabolite in tumor than in normal tissue.

† χ^2 test could not be performed because of the presence of metabolites in all samples of tumor and normal tissue.

In Vivo Results

Cho/Cr ratios were determined for patients with squamous cell carcinoma (n = 7) and healthy volunteers (n = 7). All tumors had Cho/Cr ratios greater than 1.8 (range, 1.8 to 7.2) and were above the in vitro Cho/Cr ratio corresponding to the mean Y value calculated for tumor (1.67) (Fig 10). The mean Y value for in vivo tumors (.623) corresponded to a Cho/Cr ratio of 4.2 ($10^{0.623}$) and was greater than both the cut point derived from the discriminant analysis (1.4) and the mean for in vitro tumors (1.67).

Because of differences in field strengths that affect the T1 of the tissue, acquisition parameters, potential for partial volume tissue contamination, and other intrinsic differences between our in vivo and in vitro spectroscopic techniques, it was decided that significance tests would not be appropriate. Hence, only descriptive statistics are provided. Overall, the three group means appear to be distinct, with the in vitro normal tissue having the smallest ratios, the in vitro tumor levels having higher ratios, and the in vivo tumor levels having still higher ratios (Fig 3).

No detectable Cho or Cr resonances were present in six of the seven healthy volunteers who underwent 1-D proton MR spectroscopy (Fig 11). The Cho/Cr in the one volunteer with detectable levels was 1.16, which was equal to the mean value of the Cho/Cr ratio derived for normal tissue. This would also be correctly categorized as normal tissue using the discriminant analysis classification system. These results confirm our suspicion that squamous cell carcinoma contains high Cho/Cr ratios whereas normal tissue of the extracranial head and neck does not.

Discussion

In Vitro Proton MR Spectroscopic Tissue Analysis

One-dimensional Proton MR Spectroscopy.— Elevated Cho and reduced Cr peak intensities/areas have been demonstrated in malignant lesions outside the head and neck (10, 7). Previous investigators have also shown a relative increase in the concentration of Cho with respect to Cr in malignant head and neck tumors examined in vivo (12).

The results of our 1-D proton MR spectroscopic in vitro investigation suggest that squamous cell carcinoma of the extracranial head and neck is associated with an elevation of the Cho/Cr ratio relative to muscle. A higher Cho/Cr is associated with a greater likelihood of tumor being present. By establishing a reliable tumor probability, it appears likely that this ratio may be used to help differentiate squamous cell carcinoma from nonneoplastic tissue in indeterminate masses arising in the upper aerodigestive tract.

Quantitative analysis revealed that the Cho/Cr ratios calculated for tumor and normal tissue were dependent on TE. The difference between the Cho/Cr ratios for tumor and normal tissues increased with longer TEs. These alterations with respect to TE are most likely due to relaxation effects caused by differences in T1 and T2 relaxation times, as the proton MR spectra in our study were obtained under partial relaxation conditions.

We performed fully relaxed MR spectroscopic studies on three tumor tissue samples to determine whether the differences in the in vitro Cho

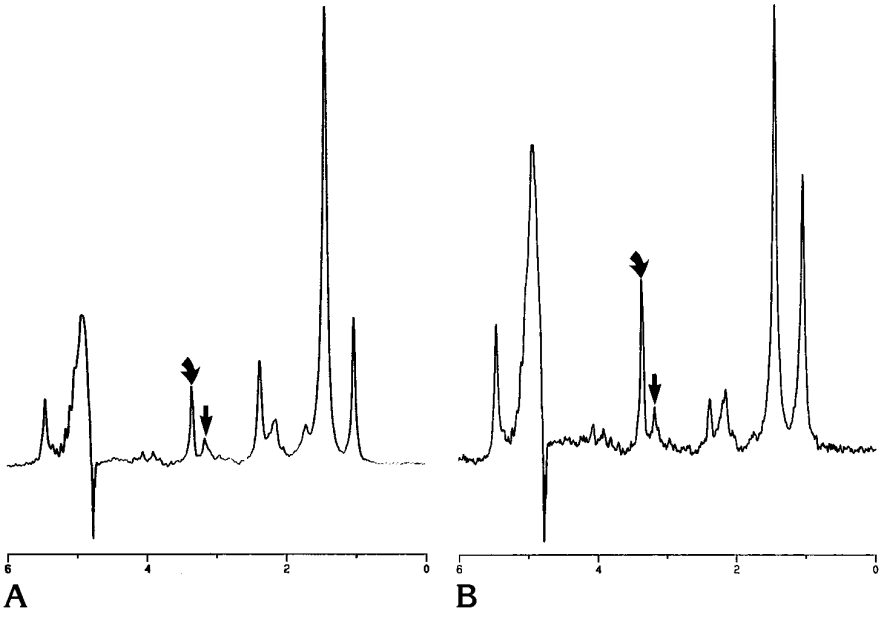

Fig 7. In vitro proton MR spectroscopy (2000/136) of squamous cell carcinoma cell line.

A, One-dimensional proton MR spectrum of squamous cell carcinoma cell culture shows elevation of Cho/Cr ratio, which measures 4.5 (*curved arrow*, Cho; *straight arrow*, Cr).

B, One-dimensional proton MR spectrum from the same sample as *A* with a TE of 272 shows elevation of the Cho/Cr ratio (5.7) relative to that seen at a TE of 136 (*A*). This increase in Cho/Cr ratio is similar to that observed in squamous cell carcinoma tissue samples (*curved arrow*, Cho; *straight arrow*, Cr).

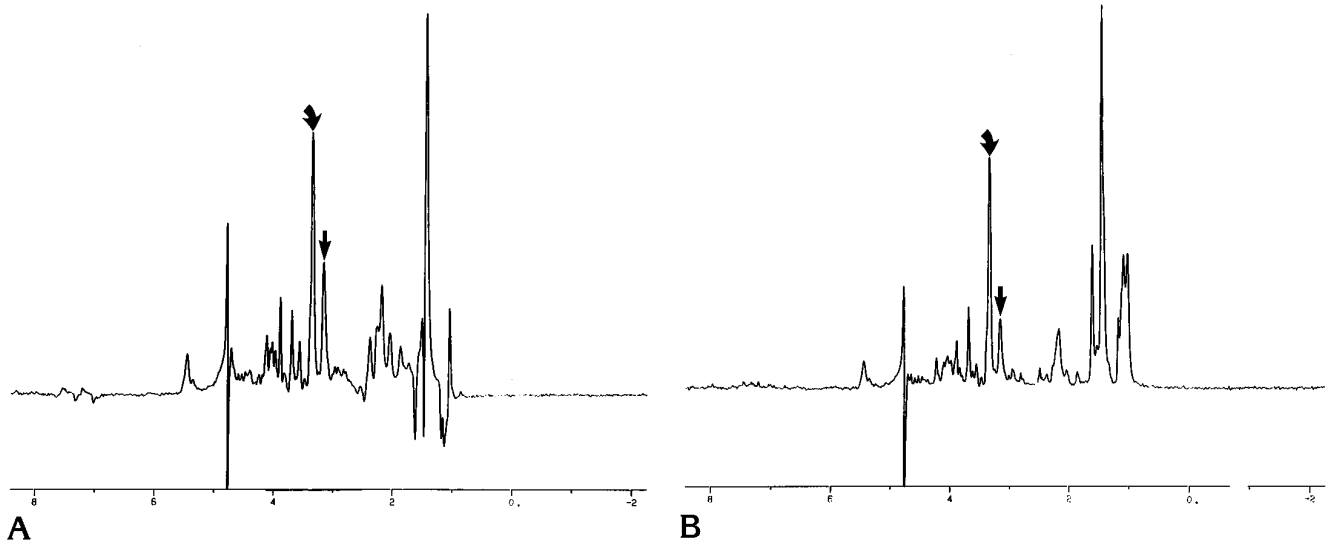

Fig 8. In vitro 1-D proton MR spectroscopy (2000/136) of metastatic cervical lymph node.

A, One-dimensional proton MR spectrum shows elevation of Cho/Cr ratio, which measures 1.98 (*curved arrow*, Cho; *straight arrow*, Cr).

B, One-dimensional proton MR spectrum obtained for same sample as in *A* but with a TE of 272 shows elevation of the Cho/Cr ratio (3.36) compared with that seen at a TE of 136 (*A*). The progressive increase in Cho/Cr ratio is similar to that illustrated previously in tissue samples of squamous cell carcinoma and cell culture (*curved arrow*, Cho; *straight arrow*, Cr).

intensities between normal tissue and tumor are due to changes in relaxation time or to concentration. We assumed a T1 of 1.5 seconds for Cho, since this is what we have found for the T1 of Cho in other cell types. To be on the safe side, we used a TR of 10 000 and performed the pulse and acquire study. No difference was observed in the relative ratios of the peak intensities as compared with the TR of 2000. Thus, the changes we found were, in all probability, due to increases in the concentration of Cho and Cr and not to changes in the relaxation time.

If the Cho/Cr ratio is to be used to detect tumor, the probability of finding a tumor will be dependent on the parameters at which the spectra were obtained. A Cho/Cr ratio of 2.0 mea-

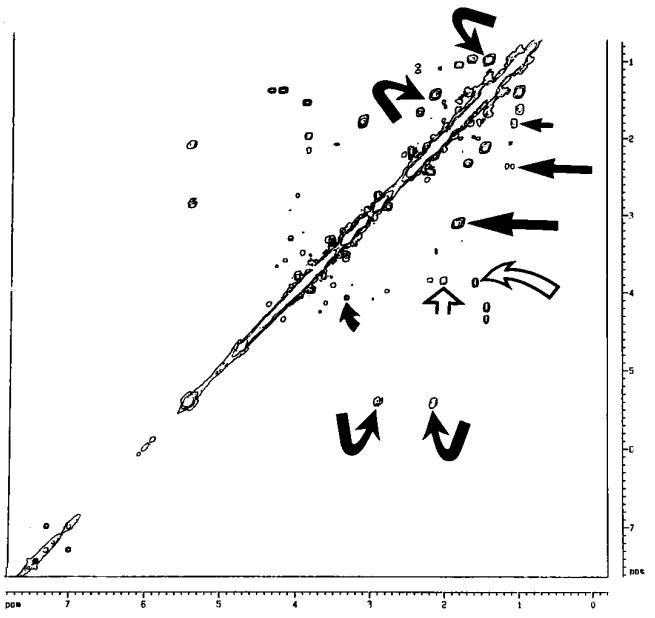

Fig 9. In vitro 2-D correlated proton MR spectrum of metastatic cervical lymph node is similar to that shown in Fig 6A. Note the presence of the specific metabolites in the current sample, which were also more likely to be detected in tumor using 2-D correlated MR spectroscopy. These metabolites include alanine (*curved open arrow*), glutathione (*straight open arrow*), histidine (*small curved solid arrow*), isoleucine (*small straight solid arrow*), valine (*medium straight solid arrow*), and shared crosspeak for polyamine/lysine (*large straight solid arrow*). Notice the absence of these metabolites in the 2-D spectrum of the normal tissue sample (Fig 6B). Note also the reduction in the chemical-shift dispersion in the triglycerides crosspeaks, similar to that seen in tumor (Fig 6A). These findings suggest that 2-D correlated MR spectroscopy may be used to detect the presence of squamous cell carcinoma within cervical lymph nodes.

sured with 2000/136 (TR/TE) was associated with a 70% probability, whereas the same ratio calculated for 2000/272 was associated with a 60% chance of finding a tumor. Similarly, tissues with a Cho/Cr ratio equal to 1.00 had a 30% probability of being tumor when measured at 2000/136 but had less than a 10% chance of being tumor when calculated at 2000/272. The shape of the probability plots also suggests that longer TEs may provide sharper discrimination between tumor and normal tissue. Although the probability function is based on a modest sample size, we think our results are promising, representing an initial step toward the establishment of guidelines for future clinical studies evaluating the ability of 1-D proton MR spectroscopy to differentiate tumor from normal tissue.

To attempt to use our in vitro results clinically, specific resonances needed to be identified that could be resolved on both small-bore high-field (11 T) and standard clinical (1.5 T) units. Although the 2-D correlated MR spectroscopic data suggest that a variety of metabolites are present in significantly higher concentrations in tumor than in normal tissue, very few of these metabolites were reliably resolved in vivo. As an example, although histidine was detectable in most tumors as compared with normal tissue, its peak was difficult to identify by 1-D proton MR spectroscopy performed at 1.5 T (10). One of the major benefits of evaluating Cho and Cr is that their 1-D spectral resonances are easily resolved on both high-field (11 T) and standard clinical (1.5 T) units. This allowed us to correlate our in vitro findings with findings obtained in a clinical setting.

A variety of other peaks were observed in our in vitro tumor spectral analysis. The exact role of these metabolites needs to be further evaluated. The large intense resonance located between 0.6 and 1.6 ppm is due primarily to fatty acids from lipids. The in vitro proton lipid spectra of normal tongue tissue (Fig 2A) had a broader spectral peak than that of squamous cell carcinoma (Fig 2B). The FWHM of the methylene group of the normal tissue was less than two times as wide as the tumor methylene linewidth. This is most likely due to intrinsic differences in relaxation between lipids present in tumors and those in normal tissue. The water shim in both cases was less than 0.1 ppm. Previous investigators have observed a similar pattern in other tumors versus normal tissue (2, 18–20). These relaxation differences between tumor and muscle triglyceride crosspeaks were also identified using 2-D correlated MR spectroscopy (Fig 6A and B).

The sharp resonance at 3.7 ppm in the tumor spectrum was not assigned (Figs 1B and 2B). In studies of colorectal tumors sampled by biopsy, Lean et al (2) observed a similar prominent resonance at 3.7 ppm. This region of the proton spectrum, namely between 3.7 and 4.0 ppm, in mammalian cells appears to contain resonances from sugars and polar headgroups of lipids. However, assignment to any one specific endogenous metabolite has not been done. Moreno et al (21) identified a sharp resonance at 3.7 ppm in MR spectra obtained in biopsy samples of colorectal tumor. They attributed this to the presence of polyethylene glycol, which is part of the lavage solution that has been absorbed by the cells in both normal and tumor tissue. However, the lavage solution used

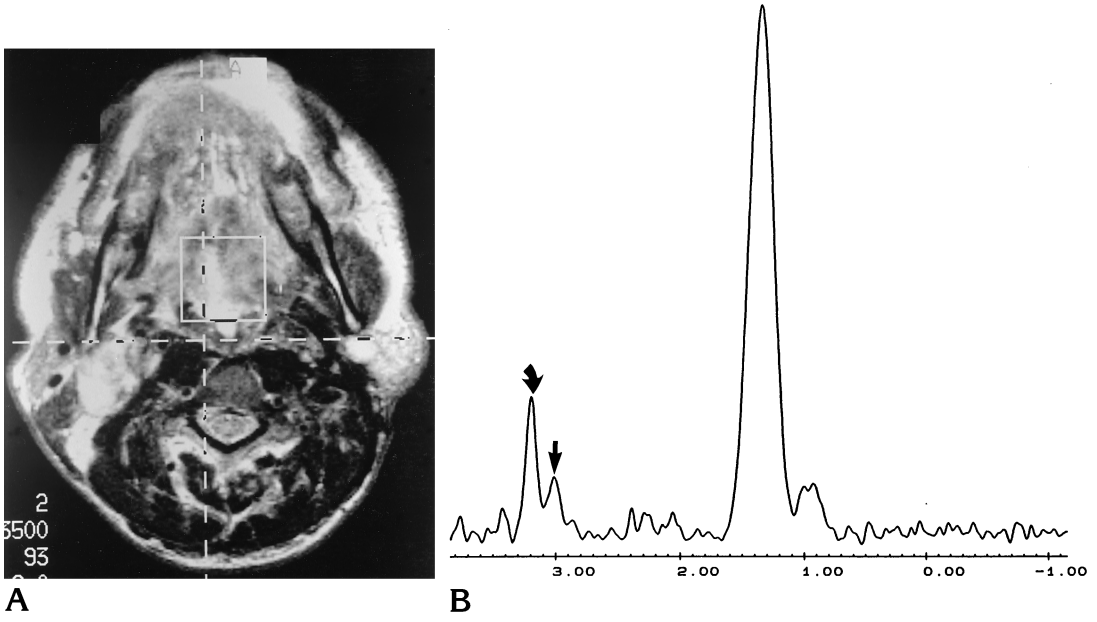

Fig 10. In vivo (1.5 T) proton MR spectroscopy (2000/136) of squamous cell carcinoma arising from the tongue base.
A, Axial T2-weighted MR image (3500/93) shows the location of the voxel seen in *B*.
B, In vivo proton MR spectrum shows elevation of the Cho peak (*curved arrow*) relative to the Cr peak (*straight arrow*). The Cho/Cr ratio was 3.33.

by our otolaryngologists is a sterile isotonic saline solution and does not contain polyethylene glycol. Thus, we were unable to assign this peak to a specific metabolite.

As expected, no peaks were observed between 6 and 8 ppm in rapidly replicating cells (Figs 1B and 2B). In this region one should only observe aromatic protons. In order to see these resonances, the unbound concentrations of these aromatic proton residues need to be in millimolar range and, if observed, the resonance peak would be very broad because of non–first-order spin-spin couplings. The aromatic protons from nucleic acid moieties should have very short relaxation times because of their lattice structure. The protons associated with the lattice should not be observable at the TEs used in our in vitro 1-D experiments.

The protons for nucleotides normally appear between 4 and 6 ppm (the resonances between 4 and 5 ppm correspond to aliphatic sugar protons, those between 5 and 6 ppm to aromatic protons). Normally, because of the pulses used to suppress the water protons, resonances between 4 and 5 ppm cannot be observed or at least cannot be assigned because they may be artifactual owing to the water-suppression pulse used. In fact, the peak at 4.7 is due to water protons not fully suppressed with the presaturation (Figs 1B and 2B).

A possible pitfall of the tissue preparation technique used in our experiments is the potential for membrane degradation, resulting in the release of high concentrations of Cho-containing compounds that are normally located within the cell membrane. The end result could be artifactual elevation of Cho, which leads to an overestimate of the actual intracellular free concentrations of Cho. The method used for sample preparation for in vitro spectroscopy is a standard technique that has been shown to minimize possible artifactual changes in in vitro spectra, including Cho elevation (2, 15, 21–26). To release this membrane/lipid associated form of Cho, phospholipases need to be activated. These phospholipases are calcium ion–dependent. The phosphate-buffered saline solution used in our experiments was a calcium- and magnesium ion–free deuterated solution, which minimizes the action of the phospholipases. In our experience in evaluating plasma cell membranes, and in that reported in the literature, the simple act of dicing tissue has not been shown to induce activation of the plasma membrane degradative processes (2, 15, 21–26).

An alternative method for tissue preparation is perchloric acid extraction. A drawback of this technique is that it can induce acid hydrolysis of membrane Cho components and, thus, increase the MR-visible level of Cho. Perchloric

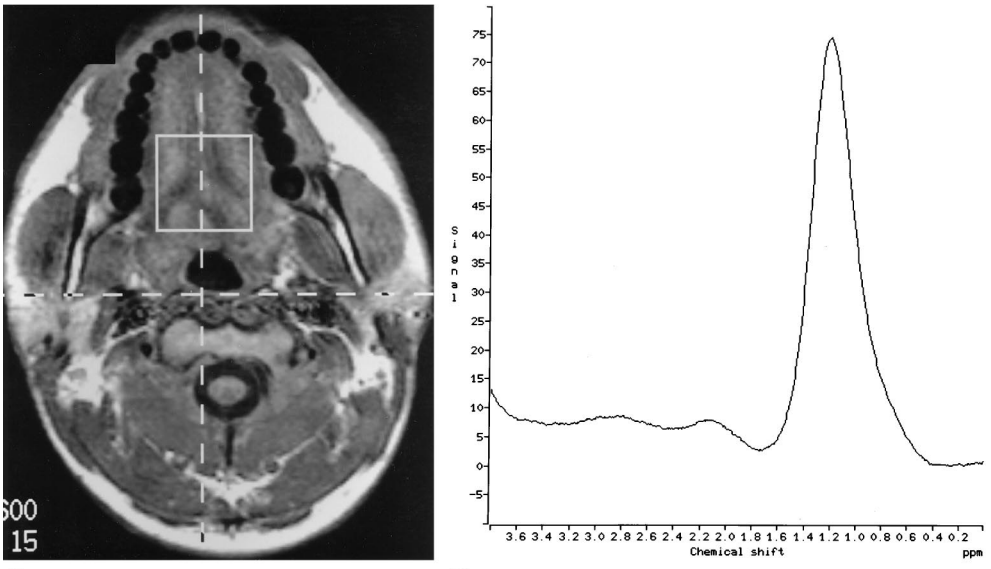

Fig 11. In vivo (1.5 T) proton MR spectroscopy (2000/136) of normal tongue base.
A, Axial T2-weighted MR image (3500/93) shows the location of the voxel seen in *B*.
B, In vivo proton MR spectrum shows no detectable levels of Cho or Cr.

acid extraction of cells is typically used if one is interested in the differences in the type of metabolites being produced and in determining "absolute" concentrations of metabolites within a cell under different conditions. We chose not to use this technique because of the potential for acid hydrolysis and the fact that this method obviously cannot be used in vivo to detect differences in metabolite levels in normal versus tumor tissue. The ultimate purpose of the 1-D in vitro MR spectroscopic studies of histologically confirmed tumors was to obtain a spectrum that would give us an idea of what we might be able to observe in an intact tumor on a whole-body clinical MR system. Our results show qualitatively similar proton spectra between in vitro and in vivo tumors (Figs 1B and 10B).

Two-dimensional Correlated MR Spectroscopy.—The results of the 2-D correlated proton MR spectral analysis demonstrated that certain amino acids and metabolites were more likely to be detected in squamous cell carcinoma than in normal tissues ($P < .05$). These amino acids and metabolites included alanine, histidine, glutathione, isoleucine, valine, and the shared crosspeak for lysine and polyamine.

The detection of certain amino acids suggests that these compounds are present in higher concentrations in tumors than in normal tissues and may be due to unregulated protein synthesis in tumors. Most likely, these metabolites are also present in normal tissues, but in such small quantities that they are not detected by 2-D correlated MR spectroscopy. The amino acids that we found to be more prevalent in squamous cell carcinoma than in normal tissue have also been reported in higher concentrations in other tumors. For example, 2-D correlated MR spectroscopic studies of colorectal and gynecologic carcinomas have revealed elevated levels of various metabolites, including the aforementioned amino acids (14, 16, 27). Delikatny et al (1) demonstrated higher levels of alanine, leucine, isoleucine, valine, and lysine in tissue samples of cervical carcinoma. Positron emission tomography with carbon-11–based compounds has also revealed an increase in amino acid metabolism in a variety of malignant lesions, including those arising in the extracranial head and neck (28, 29). Elevation in the concentration of various amino acids may be expected in tumor cells, owing to their need for more protein synthesis caused by rapid cell proliferation. Increased activity of various amino acid transport systems stemming from enhanced protein synthesis has been described in tumors (10, 30, 31). Increased amounts of alanine have been shown in meningiomas and astrocytomas (10). Additionally, accessory pathways of protein synthesis may become activated in order to meet the demands of rapid cell proliferation in tumors. For example, a less

active pathway of glutamine synthesis has been identified that allows the formation of amino acids from pyruvate, 3-phosphoglycerate, ammonium ions, and tricarboxylic acid cycle intermediates (32, 33). These findings have led some investigators to suggest the presence of this less common glutamine synthesis pathway in tumors with high alanine content (10, 33).

A number of studies have suggested that polyamines play an important role in cell proliferation and differentiation (34–36). Naturally occurring polyamines, including putrescine, spermidine, and spermine, are ubiquitous in eukaryotic organisms (34). Earlier in vitro studies have shown an increase in polyamine concentration and polyamine synthesis after viral-induced oncogenic transformation (34, 37). This increase in polyamine synthesis is thought to be due to alterations in enzymatic activity, the exact cause of which is unknown but may be due to the primary effect of oncogenic transformation with resultant increases in cellular proliferation or to a general inhibition of proteolysis resulting from oncogenic transformation (34, 37). Variations in polyamine concentration are currently being investigated as a means of assessing tumor response to chemotherapy and prognosis (34).

In our study, the 2-D correlated MR spectroscopic data analysis was performed to ascertain the presence or absence of specific metabolites. Previous reports have shown elevated levels of Cho and its derivatives in various tumors. No significant differences in Cho-based compounds between tumor and normal tissue were found by using the 2-D technique. This may in part be due to the proximity of the Cho crosspeak to the diagonal, which may make it difficult to separate this group from the diagonal. This proximity to the diagonal results from noncoupling of the methyl groups of Cho, which would be situated on the diagonal, and only very weak coupling of the methylene groups, which are located slightly off the diagonal.

Although there was no difference in the presence or absence of the various triglycerides, noticeable differences in the spectral contours of various triglyceride crosspeaks between tumor and normal tissue were observed. The contours of the various triglycerides appeared less elliptical and narrower owing to less chemical-shift dispersion in tumor as compared with normal tissue (Figs 6 and 9). This finding may be due to differences in the fluidity of mobile membrane lipids in tumor versus normal tissue (38–43). The difference in chemical-shift dispersion could also be due to changes in particular phospholipids, which can alter the fluidity of the membrane components, resulting in alterations in chemical-shift dispersion due to changes in relaxation times. Earlier studies have detected the presence of lipid structures that are highly mobile in the cell membrane of tumors as compared with similar membrane lipids analyzed from normal tissue (27, 39).

Cell Culture.—The results of the 1-D proton MR spectral analysis of cell cultures were consistent with the in vitro results obtained for tumor tissue samples. The mean Cho/Cr ratio for the squamous cell carcinoma cell culture was above the Cho/Cr ratio corresponding to the mean Y values for tumor calculated from the initial in vitro tissue study at TEs of both 136 and 272. A progressive increase in the Cho/Cr ratio associated with the lengthening of TE detected in the tissue samples was also observed in the analysis of the squamous cell carcinoma cell culture. Additionally, the ratios calculated for the cell culture on the basis of the probability curves were associated with a greater than 90% probability of tumor. The cell culture findings correlate with our in vitro results and are suggestive of rapid membrane synthesis due to increased cell proliferation.

The 2-D analysis detected the presence of only one of the six amino acids that were previously shown to be present in tumors. These differences may represent specific alterations in cellular metabolism resulting from cell transformation that may be required for in vitro growth as opposed to normal in situ growth. The fact that the polyamine/lysine shared crosspeak was present in tissue samples and cell culture suggests that this metabolite may play an important role in cellular proliferation and rapid growth.

Lymph Nodes.—The 1-D and 2-D findings show MR spectral patterns in tumor-containing lymph nodes similar to those in the in vitro cell culture and the tissue specimen analyses. The 1-D spectral analysis revealed elevation of the metastatic lymph node Cho/Cr ratios above the Cho/Cr ratio corresponding to the mean Y values for tumor calculated from the initial in vitro tissue study at TEs of both 136 and 272. Similarly, this ratio also increased with an increase in TE. The *minimum* Cho/Cr ratio detected for the three positive nodes

(1.94, 2.25) detected at TEs of 136 and 272, respectively, was associated with tumor probability of greater than 70%.

The 2-D spectral analysis showed the presence of similar metabolites to those found in our 2-D analysis of malignant tumor samples and cell culture but not detected in normal tissue. This correlation suggests that the metabolic profile found in involved nodes is due to tumor or rapidly proliferating tissue rather than being inherent to normal nodal tissue. These results also suggest that the presence of certain metabolites in cervical lymph nodes from patients with squamous cell carcinoma may be indicative of tumor involvement. Elevation of various amino acid concentrations in squamous cell carcinoma–containing nodes corresponds with the results obtained by prior investigators, who, using a colon tumor cell line, detected an elevation in amino acid concentrations in tumor-containing lymph nodes as compared with normal lymph nodes or immunostimulated nodes (15).

Our study was limited by an inability to evaluate normal and inflammatory lymph nodes, because removal of cervical nodes prior to complete histologic evaluation of the contents of the neck dissection would have interfered with staging of the tumor. Direct comparison of our results with normal and inflammatory cervical lymph nodes will be necessary before the true utility of 2-D correlated MR spectroscopy in the evaluation of cervical lymph nodes can be determined.

Our results, however, do suggest that 1-D proton MR spectroscopy may be used to determine whether lymph nodes contain tumor. This information may be useful for preoperative evaluation of cervical nodes that are indeterminate for metastases by radiographic or clinical examination, thereby directly affecting the staging and treatment of cancer. Currently, in vivo application of 1-D proton MR spectroscopy for evaluating nodal involvement is limited by the relatively large voxel size and long acquisition time required for spectral analysis at 1.5 T. Furthermore, motion artifacts caused by respiration and swallowing, both of which are inherent to neck imaging, also reduce the ability to obtain optimal proton MR spectra. The development of higher field clinical magnets and sequences that allow for reduced acquisition times may help alleviate some of these problems.

In Vivo Studies

The ratio of the concentration of Cho to Cr levels determined in vivo for tumor and normal tissue corresponded to our in vitro results. All the in vivo Cho/Cr ratios were above those corresponding to the mean Y values for tumor calculated from the initial in vitro tissue study at a TE of 136. These results were also similar to the ratio obtained from the squamous cell carcinoma cell culture. Markedly lower levels of Cho and Cr were present in the in vivo normal tissues and were consistent with previous in vivo studies of normal brain and with our in vitro analysis of normal tissue (3)(Negendank et al, "A Cooperative...''). The in vivo Cho/Cr ratio for tumor also correlated with the tumor probability curves generated from our in vitro data. The lowest Cho/Cr ratio detected for tumor in our in vivo series (1.8) was associated with a greater than 70% probability of tumor, whereas the mean Cho/Cr ratio for all tumors (4.2) was associated with a 95% tumor probability. This correlation of in vivo with in vitro results suggests that in vivo Cho/Cr ratios may be used to help detect and differentiate squamous cell carcinoma from uninvolved tissues in the extracranial head and neck.

One of the drawbacks of 1-D proton MR spectroscopy is the relatively large voxel size necessary for in vivo studies. Although the voxel size is typically smaller than that required for ^{31}P MR spectroscopy, it is still significantly larger than the size required for high-field (11 T) spectroscopy of tissue specimens. At present, a $2 \times 2 \times 2$-cm voxel (8 mL) is the smallest volume we can define using the PRESS sequence. We have performed section profile studies on phantoms to determine the size of our volumes and to estimate an out of volume fat contamination. Use of the PRESS sequence leads to defined volumes that are actually smaller by 30%. Thus, the incorporated volume is really 6.7 mL when using the defined $2 \times 2 \times 2$-cm voxel localized by the PRESS sequence. The large voxel may potentially result in contamination by normal tissue surrounding tumor, resulting in an admixture of various tissue spectra. From our previous phantom studies, we have found that if the volume abuts a fat structure, the amount of contamination from fat relative to the Cho peak is less than 10% (relative peak area determinations).

The extracranial head and neck is a difficult area to shim and we are presently accepting a

0.2 ppm water linewidth for in vivo human studies. The difficulty in shimming is due to the large magnetic susceptibility differences in this area. Incorporation of adjacent bony or air-containing structures in a large voxel reduces the likelihood of obtaining an adequate shim, resulting in a reduction of spectral resolution. In addition, the head coil we are using in these studies does not give us uniform B^1 power deposition because we are near the edge of the coil where the radiofrequency power deposition has the highest falloff. However, the results of our patient study and the correlation of these findings with the in vitro findings suggest that very little contamination was present.

The proton spectra of the normal tongue base was dominated by a broad fat resonance (0.9 to 1.3 ppm) while only a small wide resonance was present in the region of the Cho and Cr resonances (3 ppm). Because of the inherent limitations in our in vivo experiments, one could suggest that this metabolic profile of the normal tongue is artifactual in nature. We do not believe that the spectra obtained in our in vivo experiments are artifactual, since those obtained from our healthy volunteers are similar. This dominant fat resonance is indicative of the high fat concentration present in the normal tongue base. Our in vivo results also correspond to those of previous investigators. Narayana et al (42) demonstrated a similar dominant fat resonance relative to the Cho/Cr resonances in a study of human gastrocnemius muscle analyzed with proton spectroscopy at 1.5 T. The narrowing of the broad lipid resonance and elevation of the Cho/Cr ratio identified in our in vivo tumor spectra suggest replacement of high-fat-concentration tongue base muscle by squamous cell carcinoma. Further investigations using longer TEs or fat suppression may permit better in vivo resolution of Cho and Cr resonances of normal muscle (43). Additional advances that help reduce the acquisition voxel size, such as imaging on higher clinical field strength magnets or 2-D chemical-shift imaging, may also help to differentiate these resonances.

The results of this investigation revealed a qualitatively consistent pattern between the in vitro and in vivo metabolic profiles of squamous cell carcinoma as analyzed by proton spectroscopy. The elevation of the Cho peak with respect to the Cr peak and consistently narrow lipid resonances (0.9 to 1.3 ppm) were present in both the in vitro (tumor tissue samples, squamous cell carcinoma cell culture, and metastatic lymph nodes) and the in vivo experiments (Figs 1, 2, 7, 8, 10). These findings suggest that 1-D proton MR spectroscopy may be capable of differentiating squamous cell carcinoma from normal tissue and that the Cho/Cr ratio may potentially be useful in monitoring treatment. In addition, 2-D MR spectroscopy identified the presence of certain amino acids in squamous cell carcinoma that were not detected in normal tissue. These amino acids may have prognostic implications and lead to future changes in therapy. This study represents our initial experience in attempting to identify a proton MR spectroscopic metabolic profile for squamous cell carcinoma of the extracranial head and neck. Our findings should serve as a basis for further experiments that compare the Cho/Cr ratio of tumor to active inflammation, granulation tissue, scar tissue, and hematoma. Identification of the metabolic profile of these pathologic entities is one of a series of steps that must be taken before a final strategy can be defined for the clinical use of proton MR spectroscopy in the evaluation of squamous cell carcinoma of the upper aerodigestive tract.

Appendix

The validity of a *t* test or an ANOVA model depends on the distribution of the data. For these tests to be valid, the distribution of the errors in the data should follow a gaussian (normal) distribution. Careful consideration of the appropriate tests to use in analyzing the Cho/Cr area ratio (R) values (actually, the "residuals" in the analysis) led us to the conclusion that the present data were likely to violate this assumption and therefore not follow a normal distribution. Thus, standard *t* tests or ANOVA models could not be reliably performed on the R value itself. A standard strategy to rectify this situation is to perform these tests after applying a logarithmic transformation of R ($Y = \log_{10} R$). In this case, applying the logarithmic transformation permitted us to meet the assumption of a gaussian distribution of the errors, thereby helping to ensure the accuracy of the tests. Additionally, analyzing the logarithmic transform of R provides more statistical power (more sensitivity to differences) than would otherwise be obtained.

References

1. Delikatny EJ, Russell P, Hunter JC, et al. Proton MR and human cervical neoplasia: ex vivo spectroscopy allows distinction of invasive carcinoma of the cervix from carcinoma in situ and other preinvasive lesions. *Radiology* 1993;188:791–796
2. Lean CL, Newland RC, Ende DA, Bokey EL, Smith ICP, Mountford CE. Assessment of human colorectal biopsies by H-1 MRS: correlation with histopathology. *Magn Reson Med* 1993;30:525–533

3. Ott D, Henning J, Ernst T. Human brain tumors: assessment with in vivo proton MR spectroscopy. *Radiology* 1993;186:745–752
4. Kugel H, Heindel W, Ernstein R, Bunke J, duMesnil R, Friedman G. Human brain tumors: spectral patterns with localized H-1 MR spectroscopy. *Radiology* 1992;183:701–709
5. Yacoe ME, Sommer G, Peehl D. In vitro spectroscopy of normal and abnormal prostate. *Magn Reson Med* 1991;19:429–438
6. Wang Z, Sutton LN, Cnaan A, et al. Proton MR spectroscopy of pediatric cerebellar tumors. *AJNR Am J Neuroradiol* 1995;16: 1821–1833
7. Miller BL. A review of chemical issues in 1-H NMR spectroscopy: n-acetyl-L-aspartate, creatine and choline. *NMR Biomed* 1991;4: 47–52
8. Vogl T, Peer F, Schedel H, et al. 31-P spectroscopy of head and neck tumors: surface coil technique. *Magn Reson Med* 1989;7: 425–435
9. Hendrix RA, Lenkinski RE, Vogele K, Bloch, McKenna WG. 31-P localized magnetic resonance spectroscopy of head and neck tumors: preliminary findings. *Otolaryngol Head Neck Surg* 1990; 103:775
10. Kinoshita Y, Kajiwara H, Yokata A, Koga Y. Proton magnetic resonance spectroscopy of brain tumors: an in vitro study. *Neurosurgery* 1994;35:606–614
11. Mafee MF, Barany M, Gotsis ED, et al. Potential use of in vivo proton spectroscopy for head and neck lesions. *Radiol Clin N Am* 1989;27:243–254
12. Russel P, Lean CL, Delbridge L, May GL, Dowd S, Mountford CE. Proton magnetic resonance and human thyroid neoplasia. I: Discrimination between benign and malignant neoplasms. *Am J Med* 1994;96:383–388
13. McKenna WG, Lenkinski RE, Hendrix RA, Vogele K, Bloch P. The use of magnetic resonance imaging and spectroscopy in the assessment of patients with head and neck and other superficial malignancies. *Cancer* 1989;64:2069–2075
14. Lean CL, MacKinnon WB, Delikatny J, Whitehead RH, Mountford CE. Cell-surface fucosylation and magnetic resonance spectroscopy characterization of human malignant colorectal cells. *Biochemistry* 1992;31:11092–11105
15. Mountford CE, Lean CL, Hancock R, et al. Magnetic resonance spectroscopy detects cancer in draining lymph nodes. *Invasion Metastasis* 1993;13:51–57
16. May GL, Wright LC, Holmes KT, et al. Assignment of methylene proton resonances in NMR spectra of embryonic and transformed cells to plasma membrane triglyceride. *J Biol Chem* 1986;261: 3048–3053
17. Cross KJ, Holmes KT, Mountford CE, Wright PE. Assignment of acyl resonances from membranes of mammalian cells by two-dimensional NMR methods. *Biochemistry* 1984;23:407–409
18. Van Zijl PC, Moonen CT, Gillen J, et. al. Proton magnetic resonance spectroscopy of small regions (1 ml) localized inside superficial human tumors: a clinical feasibility study. *NMR Biomed* 1990;3:227–232
19. Mountford CE, Wright LC, Holmes KT, MacKinnon WB, Gregory P, Fox RM. High resolution nuclear magnetic analysis of metastatic cancer cells. *Science* 1984;226:1415
20. Bradamante S, Barchiesi E, Pilotti S, Borasi G. High resolution 1H NMR spectroscopy in the diagnosis of breast cancer. *Magn Reson Med* 1988;8:440–449
21. Moreno A, Rey M, Montane JM, et al. ^{1}H NMR spectroscopy of colon tumors and normal mucosal biopsies: elevated taurine levels and reduced polyethyleneglycol absorption in tumors may have diagnostic significance. *NMR Biomed* 1993;6:111–118
22. Halliday KR, Fenoglio-Preiser C, Sillerud IO. Differentiation of human tumors from non-malignant tissue by natural abundance C-13 NMR spectroscopy. *Magn Reson Med* 1988;7:394–411
23. Johnson M, Selinsky B, Davis M, et al. In vitro NMR evaluation of human thyroid lesions. *Invest Radiol* 1989;24:666–671
24. Mountford CE, Lean C, Mackinnon WB, Russell P. The use of proton MR in cancer pathology. In: Webb GA, ed. *Annual Reports on NMR Spectroscopy*. 1993;27:172–215
25. Sivaraja M, Turner C, Souza K, Singer S. Ex vivo two-dimensional proton nuclear magnetic resonance spectroscopy of smooth muscle tumors: advantages of total correlated spectroscopy over homonuclear J-correlated spectroscopy, *Cancer Res* 1994;54: 6037–6040
26. Russell P, Lean CL, Delbridge L, et al. Ex vivo diagnosis of potentially metastatic follicular tumors by magnetic resonance spectroscopy. *Am J Med* 1994;96:383–388
27. Ruiz-Cabello J, Cohen JS. Phospholipid metabolites as indicators of cancer cell function. *NMR Biomed* 1992;5:226–233
28. Lapela M, Grenman R, Kurki T, et al. Head and neck cancer: detection of recurrence with PET and 2-[F-18] fluoro-2-deoxy glucose. *Radiology* 1995;197:205–211
29. Lindholm P, Leskinen-Kallio S, Minn H, et al. Comparison of fluorine-18-fluoride-oxoglucose and carbon-11-methionine in head and neck cancer. *J Nucl Med* 1993;186:27–35
30. Starr MS. Uptake of taurine by retina in different species. *Brain Res* 1978;151:604–608
31. Holley RW. A unifying hypothesis concerning the nature of malignant growth. *Proc Natl Acad Sci* 1972;69:2840–2841
32. Yorek MA, Storm DK, Spector AA. Effect of membrane polyunsaturation on carrier-mediated transport in cultured retinoblastoma cells: alterations in taurine uptake. *J Neurochem* 1984;42: 254–261
33. Gill SG, Thomas DGT, Van Bruggen NV, et al. Proton MR spectroscopy of intracranial tumours: in vivo and in vitro studies. *J Comput Assist Tomogr* 1990;14:497–504
34. Sunkara PS, Baylin SB, Luk GD. Inhibitors of polyamine biosynthesis: cellular and in vivo effects on tumor proliferation. In: McCann PP, Pegg AE, Sjoerdsma A, eds. *Inhibition of Polyamine Biosynthesis: Biologic Significance and Basis for New Therapies*. Orlando, Fla: Academic Press; 1987:121–137
35. Russel DH. Clinical relevance of polyamines as biochemical markers of tumor kinetics. *Clin Chem* 1977;23:22–27
36. Cohen SS. Conference on polyamines. *Cancer Res* 1977;37:939–942
37. Don S, Bachrach U. Polyamine metabolism in normal and in virus-transformed chick embryo fibroblasts. *Cancer Res* 1975;35: 3618–3622
38. Metcalfe JC. Magnetic resonance studies of membranes and lipids. In: Wallach DFH, Fischer H, eds. *The Dynamic Structure of Cell Membranes*. Berlin: Springer-Verlag; 1971:201–228
39. Guidoni L, Mariutti G, Rampelli GM, Rosi A, Viti V. Mobile phospholipid signals in NMR spectra of cultured human adenocarcinoma cells. *Magn Reson Med* 1987;5:578–585
40. Wallach DFH. Cooperativity in biomembranes. In: Wallach DFH, Fischer H, eds. *The Dynamic Structure of Cell Membranes*. Berlin: Springer-Verlag; 1971:181–199
41. Cherry R. Protein and lipid mobility in biologic and model membranes. In: Chapman D, Wallach DFH, eds. *Biological Membranes*. London: Academic Press; 1976:47–97
42. Narayana PA, Hazle JD, Jackson EF, Fotedar LK, Kulkarni MV. In vivo 1H spectroscopic studies of human gastrocnemius muscle at 1.5T. *Magn Reson Imaging* 1988;6:481–485
43. Meyer RA. Echo acquisition during frequency-selective pulse trains for proton spectroscopy of metabolites in vivo. *Magn Reson Med* 1987;4:297–301